Fig. 5. Infrared spectra of Io (2.8 to 4.2 $\mu$m) from Cruikshank, Jones, and Pilcher (12). Note that the 4.08-$\mu$m $SO_2$ frost band is strongest at longitude 90°, where the 0.33-$\mu$m edge is strongest.



note that at orbital longitudes 290° and 307°, Io has a reflectance change at 0.4 to 0.5 $\mu$m that is greater than the change at 32°. Furthermore, at orbital longitudes $112° < \theta < 244°$, Io is relatively more reflecting shortward of 0.5 $\mu$m (that is, has a smaller reflectivity change at 0.4 to 0.5 $\mu$m relative to 32°). The variation in reflectivity shortward of 0.33 $\mu$m in the ground-based spectra is not inconsistent with the variation detected by IUE. We conclude that the relatively stronger reflectivity change between 0.4 and 0.5 $\mu$m at longitudes $290° < \theta < 307°$ is consistent with a greater fractional abundance of $S_x$ relative to $SO_2$ in that area because $S_x$ has a strong absorption between 0.4 and 0.5 $\mu$m. This interpretation derives further support from the IUE data, which show that the 0.33-$\mu$m reflectivity change (which we interpret as being due to variations in the longitudinal distribution of $SO_2$ frost) varies in the opposite sense of the 0.4- to 0.5-$\mu$m reflectivity change.

Figure 5 shows the ground-based infrared spectrum of Io at four orbital phase angles from Cruikshank et al. (12). The 4.08-$\mu$m band (due to $SO_2$ frost) is weakest at orbital phase 330° and strongest at orbital phase 90°. These data are also consistent with our hypothesis that the greatest fractional abundance of $SO_2$ frost is at longitudes greater than 29° and less than 250° and that the least abundance of $SO_2$ frost is at longitudes around 314°.

We conclude from all these data sets that the greatest fractional abundance of $SO_2$ frost is at approximate longitudes $72° < \theta < 137°$ and that those longitudes are least abundant in $S_x$. Also, longitudes $250° < \theta < 323°$ are least abundant in $SO_2$ and most abundant in $S_x$. Comparison with the Voyager color relief map in (13) shows that the longitudes where our spectrophotometric analysis finds $SO_2$ frost to be in greatest abundance are those where Io has the greatest coverage of "white" material. Furthermore, the longitudes where our analysis finds Io to be least abundant in $SO_2$ frost and most abundant in $S_x$ are those where there is substantially less white material and a greater preponderance of "red" material. We therefore conclude that the white material on Io is associated with a greater fractional abundance of $SO_2$ frost, and the red material with a greater
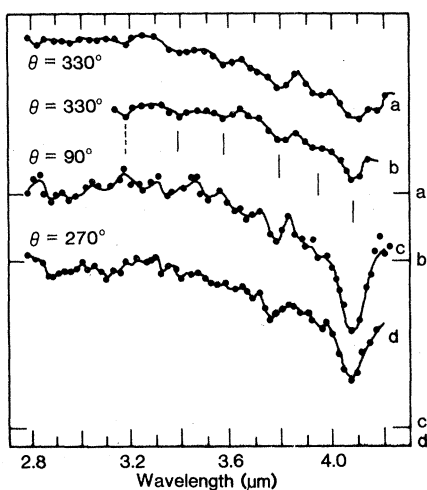
fractional abundance of other sulfurous materials.

Since volcanic activity on Io is known to be variable (13) and $SO_2$ frost deposits may originate from condensed volcanic emissions, it would not be surprising to find a major temporal as well as spatial variation in $SO_2$ frost coverage. We do not believe that most of the variation we see could be attributed to temporal changes because, to first order, inspection of the times of the spectral observations in Fig. 2, a to d, shows that the data have been repeatable as a function of orbital phase over a 15-month baseline. However, close scrutiny of the spectra (for example, L6412, L2361, L4095, and L2362) shows that the possibility of time variability cannot be completely ruled out. Because of the distinct longitudinal variation we document, the

detection of any temporal variation will need synoptic observation with very careful longitudinal control.

ROBERT M. NELSON
ARTHUR L. LANE, DENNIS L. MATSON
FRASER P. FANALE*, DOUGLAS B. NASH
TORRENCE V. JOHNSON
*Jet Propulsion Laboratory,*
*California Institute of Technology,*
*Pasadena 91103*

### References and Notes

1. W. D. Smythe, R. M. Nelson, D. B. Nash, *Nature (London)* **280**, 766 (1979).
2. F. P. Fanale, R. H. Brown, D. P. Cruikshank, R. N. Clark, *ibid.*, p. 761.
3. B. W. Hapke, *Geophys. Res. Lett.* **6**, 799 (1979).
4. D. B. Nash, F. P. Fanale, R. M. Nelson, *Bull. Am. Astron. Soc.* **11**, 597 (1979).
5. R. M. Nelson and B. W. Hapke, *Icarus* **36**, 304 (1978).
6. B. Meyer, M. Gouterman, D. Jensen, T. V. Oomen, K. Spitzer, T. Stroyer-Hansen, *Adv. Chem. Ser. No. 220* (1972).
7. C. Sagan, *Nature (London)* **280**, 750 (1979).
8. L. A. Soderblom *et al.*, *J. Geophys. Res.*, in press.
9. D. B. Nash and R. M. Nelson, *Nature (London)* **280**, 763 (1979).
10. D. L. Matson, T. V. Johnson, F. P. Fanale, *Astrophys. J.* **192**, L43 (1974); D. L. Matson, B. A. Goldberg, T. V. Johnson, R. W. Carlson, *Science* **199**, 531 (1978); R. W. Carlson, D. L. Matson, T. V. Johnson, *Geophys. Res. Lett.* **2**, 469 (1975).
11. J. B. Pollack, F. C. Witteborn, E. F. Erickson, D. W. Strecker, B. J. Baldwin, T. E. Bunch, *Icarus* **36**, 271 (1978).
12. D. P. Cruikshank, T. S. Jones, C. B. Pilcher, *Astrophys. J.* **225**, L89 (1978).
13. B. A. Smith *et al.*, *Science* **206**, 927 (1980).
14. This work represents one phase of research carried out at the Jet Propulsion Laboratory, California Institute of Technology, under NASA contract NAS 7-100. We greatly appreciate the support given to this effort by the IUE spacecraft support staff, NASA-Goddard Space Flight Center, and the resident astronomers who unselfishly supported the effort. F. C. Motteler assisted in data reduction. We acknowledge helpful comments on our manuscript by P. R. Weissman, R. W. Carlson, and W. D. Smythe.
* Present address: Planetary Geochemistry Department, Institute of Geophysics, University of Hawaii, Honolulu 96822.

16 July 1980

## 1979J2: The Discovery of a Previously Unknown Jovian Satellite

*Abstract. During a detailed examination of imaging data taken by the Voyager 1 spacecraft within 4.5 hours of its closest approach to Jupiter, a shadow-like image was observed on the bright disk of the planet in two consecutive wide-angle frames. Analysis of the motion of the image on the Jovian disk proved that it was not an atmospheric feature, showed that it could not have been a shadow of any satellite known at the time, and allowed prediction of its reappearance in other Voyager 1 frames. The satellite subsequently has been observed in transit in both Voyager 1 and Voyager 2 frames; its period is 16 hours 11 minutes 21.25 seconds ± 0.5 second and its semimajor axis is 3.1054 Jupiter radii (Jupiter radius = 7.14 × 10⁴ kilometers). The profile observed when the satellite is in transit is roughly circular with a diameter of 80 kilometers. It appears to have an albedo of ~ 0.05, similar to Amalthea's.*

Detailed examination of a wide-angle image of part of Jupiter's equatorial region (frame FDS 16383.50) taken by the Voyager 1 spacecraft 4 hours 28 minutes before its closest approach to Jupiter revealed a dark area 10 picture elements (pixels; 1 pixel $\cong 7 \times 10^{-5}$ rad) in diame-

ter that looked like a shadow (Fig. 1). The same dark area was also observed in the next wide-angle frame (FDS 16383.54), taken 192 seconds later (Fig. 2), but approximately 70 wide-angle pixels from its previous position relative to nearby atmospheric features.

The geometry of the observational situation at this time is shown in Fig. 3. The distance of the spacecraft from the dark area on the surface was approximately $4.3 \times 10^5$ km, and therefore the relative velocity of the dark area with respect to atmospheric features was approximately

13 km/sec. This velocity is two orders of magnitude larger than relative feature motion measured by Voyager 1 (*1*), so an interpretation of the image as a planetary feature could be ruled out.

The sum of the relative motion and the velocity of features due to planetary rotation indicated that the absolute velocity of the satellite throwing the shadow was approximately 26 km/sec, close to Amalthea's velocity. However, Amalthea was known not to be in a position to cause the shadow (Fig. 3). In addition, the other small satellite, 1979J1, discov-
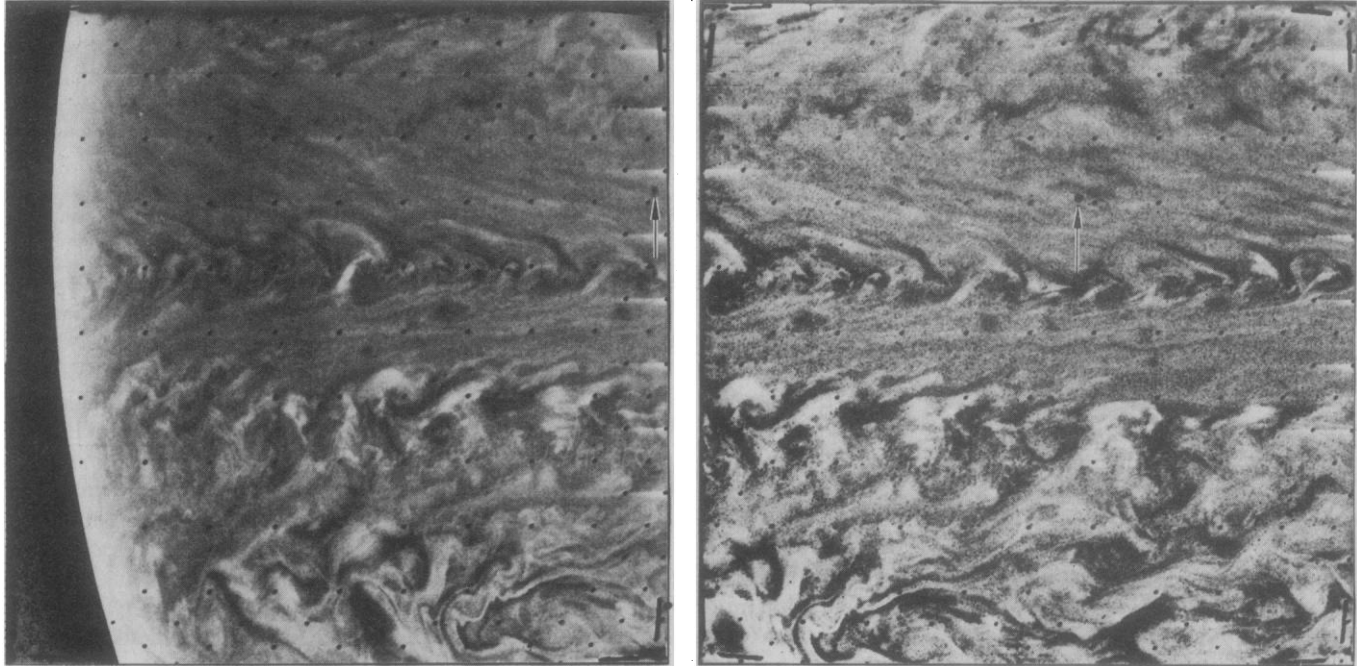


Fig. 1 (left). The first sighting of the shadow of 1979J2 occurred in this wide-angle frame (FDS 16383.50) taken by Voyager 1 at 4 hours 28 minutes before its closest approach to Jupiter. The distance from the spacecraft to the shadow on the surface is $4.3 \times 10^5$ km.       Fig. 2 (right). This wide-angle frame (FDS 16383.54) was taken 192 seconds after the frame of Fig. 1 and captured the shadow image in a different location with respect to the surrounding atmospheric features. The relative motion was approximately 70 wide-angle pixels.
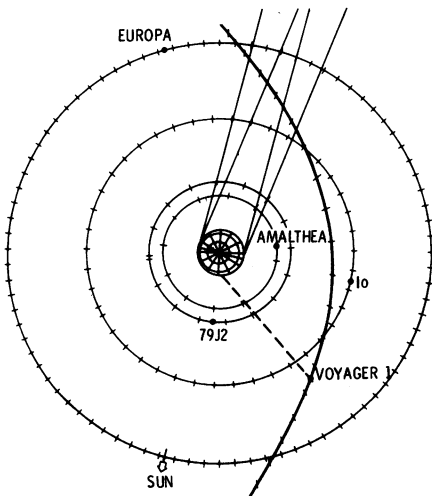


Fig. 3. Line drawing displaying the initial shadow observation geometry at about 4.5 hours before the spacecraft's closest approach to Jupiter (J − 4.5 hours). The trajectory of Voyager 1 relative to Jupiter is shown. The phase angle of Jupiter at this time is about 50°. For comparison, the orbits of Io, Europa, and Amalthea are plotted. The tick marks are at 1-hour spacing. The spacecraft and satellites are shown at the time of observation, ~ J − 4.5 hours. The dashed line shows the camera viewing direction at this time.
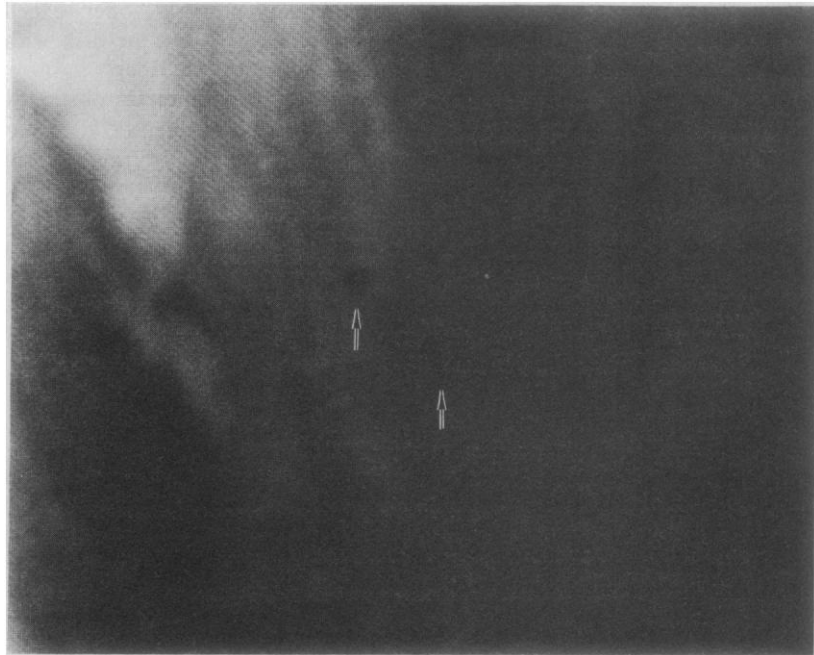
Fig. 4. Wide-angle frame (FDS 16363.45) taken by Voyager 1 at 21 hours before its closest approach to Jupiter, or approximately one orbital period of 1979J2 before the shadow observations of Figs. 1 and 2. This blowup of approximately one-tenth of the frame shows the satellite in transit against the Jovian disk and the satellite's shadow. The total extent of the satellite image in the full frame is 2 pixels. The streak near the shadow is an unrelated atmospheric feature.

ered from Voyager data (2), could be ruled out as the cause of the shadow because its greater velocity would have resulted in ~ 40 percent more motion relative to the atmosphere features than was observed.

A more detailed analysis of the two frames allowed a calculation of the orbital period as about 15 hours 45 minutes, and a search of Voyager wide-angle frames approximately 16 hours before the original shadow discovery revealed a frame (FDS 16363.45) containing images of both the satellite and its shadow (Fig. 4) in transit across the disk of Jupiter.

The satellite has now been observed in transit on images from both Voyager 1 and Voyager 2, and its period has been found to be 16 hours 11 minutes 21.25 seconds ± 0.5 second. The semimajor axis is 3.1054 Jupiter radii ($R_J$ = 7.14 × $10^4$ km). There is essentially no eccen-

tricity information to date, but an inclination of approximately 1.25° has been determined. The profile observable when the satellite is in transit is roughly circular with a diameter of about 80 km. The limited data indicate that the albedo is similar to Amalthea's, that is, about 0.05.

S. P. SYNNOTT

Jet Propulsion Laboratory,
Pasadena, California 91103

### References and Notes

1. B. A. Smith, L. A. Soderblom, R. Beebe, J. Boyce, G. Briggs, M. Carr, S. A. Collins, A. F. Cook II, G. E. Danielson, M. E. Davies, G. E. Hunt, A. Ingersoll, T. V. Johnson, H. Masursky, J. McCauley, D. Morrison, T. Owen, C. Sagan, E. M. Shoemaker, R. Strom, V. E. Suomi, J. Veverka, *Science* **206**, 927 (1979).
2. D. C. Jewitt, G. E. Danielson, S. P. Synnott, *ibid.*, p. 951.
3. This report presents the results of one phase of research carried out at Jet Propulsion Laboratory under NASA contract NAS 7-100.

17 July 1980; revised 22 September 1980

# Brightness Temperatures of Saturn's Disk and Rings at 400 and 700 Micrometers

Abstract. *Saturn was observed in two broad submillimeter photometric bands with the rings nearly edge-on. The observed brightness temperatures fall below the predictions of atmospheric models constructed from data at shorter wavelenths, indicating the presence of an opacity source besides pressure-broadened hydrogen lines in the submillimeter region. In combination with earlier measurements at larger inclination angles, these results yield a 400-micrometer brightness temperature for the rings of ~ 75 K.*

Observations at wavelengths longer than 300 μm can provide tests of current theories of the atmospheres of the giant planets. Because opacities are reduced at longer wavelengths, such observations provide temperature measurements at deeper layers in the atmosphere. In the case of Saturn, however, these measurements are hampered by the unknown emission from the rings. At submillimeter wavelengths, current telescopes cannot clearly separate the rings from the disk. The earth's passages

through the ring plane, which occur at ~ 14-year intervals, offer excellent opportunities to study the disk without interference from the rings.

We made submillimeter observations of Saturn in November 1979, when the inclination angle of the rings was only 1.2°. The observations were made at the 3-m NASA infrared telescope at Mauna Kea Observatory with the University of Chicago f/35 submillimeter photometer (1). We used a 55" focal plane aperture and two filters with spectral passbands of

300 to 800 μm (mean wavelength $<\lambda> \sim 400$ μm) and 500 to 850 μm ($<\lambda> \sim 700$ μm). The filter passbands including the effects of atmospheric transmission are shown in (1). Mars was used for calibration with an assumed brightness temperature of 211 K (2). Errors due to atmospheric extinction were reduced by alternating measurements of Saturn and Mars. We made small corrections (≤ 4 percent) to the signals from Saturn (diameter ≈ 16") to correct for the partial resolution of the planetary disk by using beam scans measured on Mars (diameter ≈ 7"). Saturn brightness temperatures were derived from the observed signals by the procedures outlined by Loewenstein et al. (3). The results are shown in Table 1.

An increase in temperature with wavelength in the submillimeter region is a feature common to all planetary atmosphere models for Saturn. Our 400-μm brightness temperature is in good agreement with profile C derived by Gautier et al. (4); however, the model predicts a 700-μm temperature greater than 150 K. Their model N, which gives a better fit to mid-infrared limb scans (5), predicts substantially higher temperature at both wavelengths. The Gautier et al. models are derived from observations in the far-infrared ( 20 to 200 μm), where the dominant opacity is due to pressure-broadened $H_2$ lines. In the submillimeter region there may be additional sources of opacity that would lower the brightness temperatures predicted by the models. Klein et al. (6) calculated models including opacity due to $NH_3$, which appear to give lower submillimeter temperatures; unfortunately, these models have been calculated only for λ > 1 mm. Clouds of $NH_3$ ice crystals (7) may also be an important source of opacity at submillimeter wavelengths. Our results seem to require an opacity source besides the pressure-broadened $H_2$ lines; models specifically related to the submillimeter region are needed.

The measurements reported here can be combined with earlier observations at larger ring inclination angles (≳ 20°) to estimate the submillimeter brightness of the rings. The presence of the rings affects the total submillimeter flux in two ways, through thermal emission from the rings themselves and through attenuation of the disk radiation where the rings overlap the disk. To calculate the emission from the rings, we assume that the A and B rings are equally bright and that they radiate as a Lambertian surface with a brightness temperature $T_R(\lambda)$. We calculate the attenuation of the disk radiation by assuming a wavelength-inde-

Table 1. Summary of Saturn observations.

| Mean wavelength (μm) | Date (U.T. 1979) | Flux density ratio* (Saturn/Mars) | Surface brightness ratio† (Saturn/Mars) | Brightness temperature‡ (K) |
|---|---|---|---|---|
| 400 | 27 November | 2.56 ± 0.08 | 0.535 | 121 |
|  | 28 November | 2.56 ± 0.08 | 0.540 | 122 |
|  | Mean |  |  | 121 ± 12 |
| 700 | 27 November | 3.03 ± 0.09 | 0.633 | 137 |
|  | 28 November | 3.09 ± 0.09 | 0.652 | 141 |
|  | Mean |  |  | 139 ± 15 |

*The observed signal ratio has been increased by 2 percent at 400 μm and 4 percent at 700 μm to correct for partial resolution of Saturn's disk. †Both planets are assumed to be uniformly bright. ‡The errors in brightness temperature are dominated by the 10 percent uncertainty in the assumed martian temperature (211 K). Other sources of error are the uncertainty in the resolution correction (2 percent), statistical uncertainties (≲ 1 percent), and the differences between the two nights (< 3 percent).